polysaccharides

MDPI

Article

Influence of the Purification Degree of Cellulose from *Posidonia oceanica* on the Properties of Cellulose-PLA Composites

Paula Camarena-Bononad, Pedro A. V. Freitas *, Chelo González-Martínez, Amparo Chiralt and Maria Vargas *

Instituto de Ingeniería de Alimentos-FoodUPV, Universitat Politècnica de València, 46022 Valencia, Spain; paucabo@doctor.upv.es (P.C.-B.); cgonza@tal.upv.es (C.G.-M.); dchiralt@tal.upv.es (A.C.)
* Correspondence: pedvidef@doctor.upv.es (P.A.V.F.); mavarco@tal.upv.es or mavarco@upv.es (M.V.)

Abstract: PLA biocomposites, incorporating 5% wt. of lignocellulosic fibres (LF) from *Posidonia oceanica* waste with different degrees of cellulose purification, were obtained by melt blending and compression moulding. The LF were obtained after removing part of the non-cellulosic components by subcritical water extraction at 150 and 170 °C and after bleaching the extracted residues with hydrogen peroxide or sodium chlorite. The non-bleached LF provided the composites with a brown colour and opacity, while the bleached LF impacted the optical properties of composites to a lower extent, depending on their whiteness. The LF composition had a noticeable effect on the composites' mechanical and barrier properties. All LF reduced the water vapour barrier capacity while promoting the oxygen barrier of the films. Bleached LF enhanced the film stiffness and reduced extensibility and resistance to break, whereas non-bleached LF had lower impacts on the tensile parameters. Considering the mechanical and barrier performance of the composites, the fibres obtained at 170 °C and bleached with sodium chlorite exhibited the best behaviour. Nevertheless, if transparency and colour are not limiting for the use of the films, untreated LF allowed for good preservation of the water vapour permeability of PLA films and enhanced the oxygen barrier capacity, with a similar mechanical response as the other non-bleached fractions.

Keywords: biocomposites; lignocellulosic fractions; tensile behaviour; barrier properties; colour; transparency

Citation: Camarena-Bononad, P.; Freitas, P.A.V.; González-Martínez, C.; Chiralt, A.; Vargas, M. Influence of the Purification Degree of Cellulose from *Posidonia oceanica* on the Properties of Cellulose-PLA Composites. *Polysaccharides* **2024**, *5*, 807–822. https://doi.org/10.3390/polysaccharides5040050

Academic Editor: Adrian C. Puiţel

Received: 7 October 2024
Revised: 15 November 2024
Accepted: 3 December 2024
Published: 5 December 2024

1. Introduction

Posidonia oceanica (PO) is a seagrass endemic to the Mediterranean Sea, forming extensive meadows from the surface to depths of 40 m [1]. It is essential due to its high primary production [2] and its contributions to structuring and diversifying marine habitats [3]. Nevertheless, various human factors can negatively affect the PO's ecosystem, including trawling, sewage discharges, and coastal modifications [4]. Likewise, natural factors, such as their life cycle and the actions of waves, air currents, and winds, can also impact the existence of PO. Both human and natural factors can cause the detachment of the plant from the meadows and accumulate on the seashore, which leads to the formation of accumulations up to 4 m high that have to be removed from beaches for recreational and tourist purposes [5,6]. In this sense, every year, a large amount of PO waste is removed from the beaches and disposed of in landfills without being appropriately used. This underutilisation of a resource-rich waste stream not only generates a cost but also leads to significant losses of organic matter, which makes it urgent to find environmentally friendly alternatives for its correct use. Previous studies have shown that the leaves of PO waste contain polysaccharides with high added value, mainly cellulose (31–40%) and hemicellulose (21–35%), and other types of organic polymers such as lignin (26–30%) [7–10]. Therefore, this lignocellulosic waste can be considered a good source of cellulose with many applications in different fields, including the packaging sector [11].

In lignocellulosic residues, the close polymeric alignment of cellulose chains and its interactions with hemicellulose and lignin structures give them recalcitrant properties. Therefore, obtaining cellulose from these residues involves different physical and chemical treatments, which usually implies a great amount of toxic and corrosive compounds that are critical to reduce in order to apply a greener and more sustainable process [12]. Recently, Camarena-Bononad et al. [7] obtained cellulose fibres from PO by applying a more environmentally friendly process combining subcritical water extraction and subsequent bleaching using hydrogen peroxide in an alkaline medium, with good yield (24–25 g of purified fibres/100 g of PO) and cellulose purity (85%).

Subcritical water extraction (SWE) is a green method that can fractionate lignocellulosic components with preserved molecular functionalities and high molecular weights [13]. Subcritical water is liquid water at temperature and pressure below its critical point (374.15 °C and 22.1 MPa) [14]. Under subcritical conditions, the water shows a decrease in its dielectric constant and viscosity, which, combined with high extraction temperatures and pressures, has a high penetrating power in the plant tissue, hydrolysing some chemical bonds and facilitating cellulose recovery from the lignocellulosic matrix. Water as a solvent, in addition, is highly available and cheap; it allows the extraction of polar and non-polar compounds, and the extraction time is shorter, thus being more efficient and eco-friendlier than other traditional extraction methods [15]. Likewise, bleaching treatments are applied to the lignocellulosic materials for their delignification, enhancing the hydrolysis and removing the remaining hemicelluloses [16]. In general, chlorine-based solvents, such as sodium chlorite ($NaClO_2$), are used for cellulose bleaching treatments. $NaClO_2$ in an acidic buffer solution breaks down into chlorine dioxide (ClO_2), which can oxidise the remaining lignin by attacking the aromatic rings present in its structure [17]. Treatments based on oxygen derivatives like hydrogen peroxide (H_2O_2) can be used as an alternative to chlorine bleaching methods. Specifically, H_2O_2 dissociates into perhydroxyl anions (HOO^-), which have high bleaching power [18]. Hydrogen peroxide has proven to be a highly efficient and competitive bleaching agent due to its delignification efficiency, low cost, and reduced environmental impact [18,19].

The conventional plastics used for food packaging are mostly non-biodegradable or compostable and obtained from non-renewable resources, causing major environmental and disposal issues worldwide. Their substitution by biodegradable polymers from renewable resources has attracted growing interest from industries and researchers as a solution to environmental problems [20]. Poly (lactic acid) (PLA) is a thermoplastic polymer obtained from renewable resources that exhibits high strength and rigidity. At the same time, PLA is compostable and biocompatible/bioabsorbable, with potential applications in different industrial and medical fields. Therefore, this polymer offers a technical and viable alternative to the environmentally harmful problem caused by the accumulation of non-degradable plastics [21].

Incorporating fillers or reinforcing agents from renewable resources has been extensively studied to improve or modulate the functional properties of biodegradable materials, lowering their cost [22–24]. Biopolymer-based composites (biocomposites) are eco-friendly and sustainable materials that are interesting for several applications. These contain natural fibres and biodegradable polymers, such as PLA. The biocomposites based on PLA are entirely bio-based materials with promising biodegradability and mechanical properties since their biodegradability is enhanced by increasing the fibre content [22,25]. Different studies have explored their potential to substitute petroleum-based products [22–24], numerous studies have already used different natural fibres to obtain PLA biocomposites with modulated properties for different purposes, and further research and development are needed for the cost reduction and broader utilisation of PLA biocomposites. Specifically, PLA biocomposites with ground PO waste leaves of different particle sizes at different ratios have been characterised as to their different properties [26–28]. Likewise, fibres from PO waste balls have also been incorporated into injection-moulded PLA composites [29,30]. However, no previous studies have analysed the influence of the different degrees of

cellulose purification from *Posidonia oceanica* waste, applying different treatments, on the properties of PLA composite films for packaging applications.

In biocomposite development, fibre modification by applying surface treatments with different chemicals (alkali, silane, or coupling agents) or physical treatments (plasma, ultrasound, ultraviolet, and ozone treatments) can improve the fibre–polymer interactions at the interface, improving the interfacial adhesion [31], which can provide biocomposites with properties to match different requirements. Nonetheless, using lignocellulosic fractions with different degrees of cellulose purification could be an interesting, low-cost alternative to cellulose modifications to obtain reinforced composite films. The different lignocellulosic components could affect the degree of interfacial entanglement of the fibre–polymer network, thus improving the force transferring from the fibres to the polymer matrix. The reduction of the use of chemicals to produce natural fibres is a challenge within the principles of sustainable chemistry. A comparison of the properties of composites containing fibres obtained by different treatments would allow for selecting a greener method that produces adequate performance of the composite for a determined application.

This study aimed to obtain and characterise PLA biocomposites using PO lignocellulosic fractions with different degrees of cellulose purification to obtain low-cost reinforced food packaging materials. In this sense, the lignocellulosic PO fractions were obtained after subcritical water extraction (at 150 and 170 °C) and subsequent bleaching treatments with sodium chlorite or different concentrations of hydrogen peroxide (4 and 8%). The raw PO powder, the SWE residues, and the different bleached fractions were used to obtain PLA biocomposites by melt blending and compression moulding. These films were characterised for their structural, optical, barrier, tensile, and thermal properties.

2. Materials and Methods

2.1. Materials

Amorphous PLA 4060D with a density 1.24 g.cm^{-3}, an average molecular weight of 106,226 D, and a 40% low molecular weight fraction (275D) was supplied by Natureworks (Plymouth, MN, USA). Hydrogen peroxide (H_2O_2, 30%), sulphuric acid (H_2SO_4, 98%), acetic acid, di-phosphorus pentoxide (P_2O_5), and magnesium nitrate ($Mg(NO_3)_2$) were supplied by PanReac Quimica S.L.U. (Castellar del Vallés, Spain). Sodium chlorite ($NaClO_2$), sodium hydroxide (NaOH), sodium acetate, glucose, and arabinose were obtained from Sigma-Aldrich (St. Louis, MO, USA). D(+)-Xylose was purchased from Merck KGaA (Darmstadt, Germany).

2.2. Lignocellulosic Fractions

The lignocellulosic fibres from PO were obtained, as reported by Camarena-Bononad et al. [7], and used to prepare the PLA composite films. Briefly, PO waste was supplied by a landfill located in Denia (Alicante, Spain). As shown in Figure 1, after the leaves were separated from the rest of the uninteresting components, PO leaves were washed, dried (50 °C for 72 h), milled (Model SM300 stainless, Retsch GmbH, Haan, Germany), and sieved to obtain particles under 0.50 mm. Afterwards, the PO was submitted to two different subcritical water extraction (SWE) conditions (150 °C, 5 bar; 170 °C, 9.5 bar; both for 30 min), obtaining two insoluble lignocellulosic residues (fibres 150 and 170, respectively). Then, for each insoluble residue, three bleaching treatments were used to purify the cellulose: (1) and (2) using H_2O_2 at two concentrations, 4 and 8% (*v*/*v*), at pH 12 for 4 cycles of 1 h each; and (3) using $NaClO_2$ (1.7% wt.) at pH 4.5, for 5 cycles of 4 h each. From these bleaching treatments, 6 cellulosic fibres were obtained, as shown in Figure 1: 150-4, 170-4, 150-8, 170-8, 150-C, and 170-C. Every lignocellulosic residue was dried in a vacuum oven (S. P. Selecta, s. a., Barcelona, Spain) at 60 °C for 3 days, ground (IKA, model M20, Staufen, Germany), and sieved to eliminate particles bigger than 125 µm. They were conditioned in a desiccator containing P_2O_5 (0% RH) until further use. The chemical composition of the different dry fibres, determined according to the NREL/TP-510-42618-2008 method [32], are shown in Table 1 in terms of the structural components (cellulose, hemicellulose, and

lignin) and ash content, as reported in a previous study [7]. The content of bonded water, determined by TGA through the weight loss at 120 °C, is also shown in Table 1.

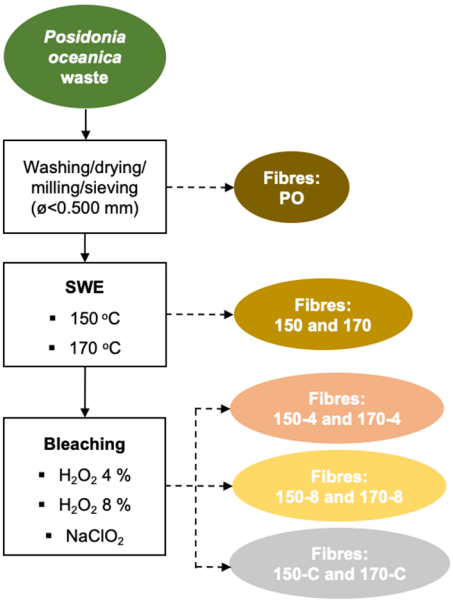

Figure 1. Flow chart of the process applied to obtain different lignocellulosic fibres from *Posidonia oceanica* waste.

Table 1. Weight percentage * of bonded water (determined by TGA), ashes, and structural components (cellulose, hemicellulose and lining) of the different lignocellulosic fibres used as fillers for PLA films.

Fibre Sample	Bonded Water *	Cellulose *	Hemicellulose *	Lignin *	Ashes *
PO	8.7 ± 0.0	29.6 ± 0.6	8.9 ± 0.4	13.6 ± 0.3	20.0 ± 0.3
150	6.7 ± 0.3	39.0 ± 4.0	10.6 ± 1.0	20.6 ± 1.2	8.4 ± 0.2
170	5.7 ± 0.2	51.1 ± 0.7	4.6 ± 0.1	23.5 ± 0.4	10.3 ± 0.3
150-4	8.5 ± 0.9	67.0 ± 5.3	19.8 ± 0.8	9.6 ± 0.7	10.8 ± 0.7
170-4	6.7 ± 1.1	79.6 ± 2.8	8.8 ± 0.1	10.2 ± 0.1	10.4 ± 0.0
150-8	5.6 ± 2.2	69.8 ± 1.2	17.9 ± 1.6	7.7 ± 0.4	12.5 ± 0.2
170-8	6.8 ± 2.5	84.6 ± 1.0	7.7 ± 0.2	10.0 ± 0.2	4.9 ± 1.1
150-C	4.7 ± 1.3	90.4 ± 1.6	7.0 ± 0.5	3.7 ± 0.7	1.4 ± 0.2
170-C	2.8 ± 0.0	95.1 ± 0.9	2.9 ± 0.7	3.4 ± 0.9	1.7 ± 0.4

* Data from Camarena-Bononad et al. [7].

2.3. Film Preparation

Green PLA composite films with 5% of wt. of different lignocellulosic fractions were prepared by melt blending and compression moulding. The fibre ratio was chosen within the range usually incorporated in composite films [33]. Amorphous PLA was selected on the basis of its better heat-sealing properties than semicrystalline PLA. Firstly, PLA pellets were dried at 60 °C for 24 h in a vacuum oven (S. P. Selecta, s. a., Barcelona, Spain) to eliminate the residual water. The dried PLA pellets were previously mixed in a beaker with the different lignocellulosic fractions conditioned at 0% relative humidity in desiccators containing P_2O_5, and then melt-blended using an internal mixer (HAAKETM PolyLabTM QC, Thermo Fisher Scientific, Karlsruhe, Germany) at 160 °C and 50 rpm for 6 min. After that, the solid blend was cold milled using a gridding machine (IKA, model M20, Germany), and films were thermoformed for the different milled blends (4 g per film) using a hydraulic press (Model LP20, Labtech Engineering, Thailand), applying preheating at 160 °C for 3 min, compression at 100 bar at 160 °C for 3 min, and finally cooling to 70 °C. As a control formulation, PLA films without cellulosic fractions were prepared. The next ten formulations based on PLA were obtained: without lignocellulosic fractions (PLA) and with each one of the cellulosic fractions that was coded based on the fibre name PO, 150,

170, 150-4, 170-4,150-8, 170-8, 150-C, and 170-C. All films were conditioned at 0 or 53% RH at 25 °C for at least one week before the analyses.

2.4. Film Characterisation

2.4.1. Optical Properties

The optical properties of the films conditioned at 53% RH were analysed according to the Kubelka–Munk theory of multiple scattering [34]. The reflection spectra (R) of the films from 400 to 700 nm, obtained on white (R_g) and black (R_0) backgrounds, were determined using a spectrocolorimeter (CM-3600d, Minolta Co., Tokyo, Japan). The internal transmittance (T_i) and the infinite reflectance (R_∞) were obtained according to Equations (1)–(4). The film colour coordinates L^* (lightness), a^* (redness–greenness), and b^* (yellowness–blueness) were obtained from the R_∞ spectra, considering illuminant D65 and 10° observer. Then, the psychrometric colour coordinates, chroma ($C_{ab}{}^*$), hue angle ($h_{ab}{}^*$), and total colour difference (ΔE^*) with respect to the net PLA film were obtained using Equations (5)–(7). The measurements were carried out in triplicate for each formulation.

$$T_i = \sqrt{(a + R_0)^2 - b^2} \quad (1)$$

$$R_\infty = a - b \quad (2)$$

$$a = \frac{1}{2}\left[R + \left(\frac{R_0 - R + R_g}{R_0 \times R_g}\right)\right] \quad (3)$$

$$b = \sqrt{a^2 - 1} \quad (4)$$

$$h^*_{ab} = arctg\left(\frac{b^*}{a^*}\right) \quad (5)$$

$$C^*_{ab} = \sqrt{a^{*2} + b^{*2}} \quad (6)$$

$$\Delta E^* = \sqrt{\left(\Delta L^*\right)^2 + \left(\Delta a^*\right)^2 + \left(\Delta b^*\right)^2} \quad (7)$$

where $\Delta L^* = \left(L^* - L^*_0\right)$; $\Delta a^* = \left(a^* - a^*_0\right)$; $\Delta b^* = \left(b^* - b^*_0\right)$; and L^*_0, a^*_0, and b^*_0 are the colour coordinates of the control PLA film without cellulosic fractions.

2.4.2. Barrier Properties

The water vapour permeability (WVP) of the films conditioned at 53% RH was determined according to ASTM E96/E96M [35]. For this, film samples were cut (Ø = 3.5 cm) and placed and sealed in Payne permeability cups previously filled with 5 mL of distilled water (100% RH). The cups were placed into desiccators containing an $Mg(NO_3)_2$ over-saturated solution (53% RH) at 25 °C and weighed periodically using an analytical balance (ME36S, Sartorius, ±0.00001 g, Fisher Scientific, Hampton, NH, USA) every 2 h for 64 h. The WVP was calculated from the slope of the weight loss–time curves. The measurements were performed in triplicate.

The oxygen permeability (OP) of the films conditioned at 53% RH was determined using an Oxygen Permeation Analyzer (Model 8101e, Systech Illinois, IL, USA) at 25 °C and 53% RH, according to ASTM D3985-05 [36]. For this, the oxygen transmission rate (OTR) through the films with an exposure area of 50 cm^2 was determined every 15 min until equilibrium was reached. The OP of the films was calculated by considering the OTR, film thickness, and difference in partial pressure of oxygen between the two sides of the films. For each formulation, the measurements were taken in duplicate.

2.4.3. Thickness and Tensile Properties

A digital micrometre (Palmer, model COMECTA, Barcelona, Spain, accuracy of 0.001 mm) was used to measure the film thicknesses at ten random film positions.

The tensile properties of the films conditioned at 53% RH were obtained according to ASTM D882 [37] using a universal testing machine (Stable Micro Systems, TA.XT plus, Stable Micro Systems, Godalming, UK). The films were cut (25 × 100 mm) and placed between two grips initially separated by 50 mm and stretched at a crosshead speed of 50 mm·min^{-1}. The elongation at break (EB), tensile strength at break (TS), and elastic modulus (EM) of the films were determined. Eight samples were evaluated for each formulation.

2.4.4. Thermal Properties

The thermal stability of the films conditioned at 0% RH was analysed in duplicate using a thermogravimetric analyser (TGA 1 Stare System analyser, Mettler-Toledo, Greifensee, Switzerland). The films were previously conditioned in a desiccator containing P_2O_5 at 25 °C for two weeks. Samples of about 3–5 mg were weighed and heated from 25 to 900 °C under a constant flow of nitrogen (10 mL·min^{-1}) at 10 °C min^{-1}. The weight loss vs. temperature and their corresponding derivative (DTGA) curves were obtained using the STARe Evaluation Software (version V12.00a, Mettler-Toledo, Inc., Greifensee, Switzerland).

Differential scanning calorimetry (DSC) was used to determine the phase transitions of the films using a DSC Stare System analyser (Mettler-Toledo GmbH, Greifense, Switzerland). Samples conditioned at 0% RH were sealed in aluminium pans (5–7 mg) and heated from −25 to 200 °C at a heating rate of 10 °C ·min^{-1}, maintained at 200 °C for 5 min, cooled to −10 °C at −50 °C·min^{-1}, maintained at −10 °C for 5 min, and heated again to 200 °C at a heating rate of 10 °C·min^{-1}. The analysis was performed in duplicate for each film formulation.

2.4.5. Microstructural Properties

A high-resolution field emission scanning electron microscope (HRFESEM, GeminiSEM 500, Zeiis, Oxford Instruments, Oxford, UK) was used to observe the cross-sections of the films conditioned at 0% RH. Before the observation, films were immersed in liquid nitrogen and cryo-fractured and coated with platinum using an EM MED020 sputter coater (Leica BioSystems, Barcelona, Spain). The images were taken at ×400 magnification (with inserts at ×2000) using an acceleration voltage of 1.5 kV.

2.5. Statistical Analysis

Analysis of variance (ANOVA) was carried out to study the effect of the incorporation of different lignocellulosic fractions in PLA-based films using Statgraphics Centurion XIX and considering the least significant difference of 95% ($\alpha = 0.05$).

3. Results and Discussion

3.1. Optical Properties of the Films

Figure 2 shows the visual appearance of the different PLA films. A naked-eye observation shows that the transparency and colour characteristics of the PLA films with the different lignocellulosic fibres differ greatly due to the presence of solid particles with different purification degrees. The films that differ the least from the PLA control would be those prepared with PLA and chlorite-bleached fibres because these are the cellulose fibres that have the highest whiteness index and cellulose purity (Table 1). This was reflected in the values of the total colour difference (ΔE^*) shown in Table 1 for the net PLA film. Similar optical characteristics were observed in PLA films containing PO cellulose nanofibers [38].

Table 2 also shows the colour coordinates (L^*, $C_{ab}{}^*$, and $h_{ab}{}^*$) of the different films and the respective whiteness index (WI) of the fibres. Every lignocellulosic material reduced the film lightness (L^*) while promoting an increase in colour saturation and conferring a yellowish hue to the films. L^* decreased in films prepared with PO and the lignocellulosic fraction obtained from the SWE treatment (150 and 170), and increased in films prepared with chlorite-bleached residues. Of the bleached residues, those treated with sodium chlorite provoked the lowest colour difference, while those treated with 4% H_2O_2 exhibited the most significant colour difference. Likewise, the fibres processed at 170 °C always

caused the greatest colour difference, according to the different levels of the WI of the fibres. Good linear correlations of the film lightness (L^*) and hue (h_{ab}^*) values with the WI of fibres were obtained, and the r-values were 0.965 and 0.931, respectively. Therefore, the WI of the fibres greatly impacted the film's lightness and chromatic appearance.

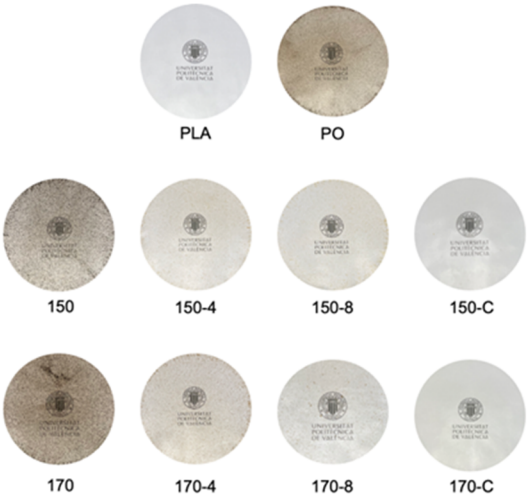

Figure 2. Visual appearance of the PLA films with the different lignocellulosic fibres incorporated.

Table 2. Colour coordinates and total colour difference (ΔE^*) of the different PLA films with the incorporated lignocellulosic fibres with different whiteness index (WI) values.

Formulation	L^*	C_{ab}^*	h_{ab}^*	ΔE^*	WI [(1)]
PLA	68.1 ± 0.4^{h}	4.7 ± 0.1^{a}	27.5 ± 5.7^{a}	0.0	-
PO	36.7 ± 1.5^{c}	8.6 ± 0.1^{b}	68.1 ± 0.3^{c}	32.0	40.9
150	34.4 ± 2.2^{b}	5.2 ± 0.0^{a}	64.9 ± 0.6^{b}	33.8	29.7
170	29.9 ± 1.2^{a}	4.6 ± 0.3^{a}	63.9 ± 0.6^{b}	38.3	27.8
150-4	58.6 ± 1.4^{e}	16.7 ± 0.9^{e}	72.7 ± 0.4^{d}	16.8	65.6
170-4	49.0 ± 0.5^{d}	13.7 ± 0.1^{c}	68.2 ± 0.4^{c}	21.9	57.4
150-8	63.3 ± 0.7^{f}	15.4 ± 0.5^{d}	81.5 ± 0.4^{e}	14.0	67.8
170-8	61.3 ± 0.5^{g}	15.8 ± 0.6^{d}	77.7 ± 0.1^{f}	15.0	60.6
150-C	70.2 ± 0.3^{i}	8.0 ± 0.4^{b}	84.3 ± 0.7^{fg}	7.0	91.7
170-C	70.1 ± 0.1^{i}	8.5 ± 0.3^{b}	85.0 ± 0.5^{g}	7.4	88.7

[(1)] Whiteness index values determined in the fibres [7]. Different letters in the same column indicate significant differences among the samples ($p < 0.05$).

The film transparency is reflected in the internal transmittance (T_i) spectra shown in Figure 3. Incorporating fibres into the PLA films reduced the film transparency to different extents, depending on the cellulose purification degree. T_i decreased to a lower extent with the whitest fibres (chlorite-bleached), which did not show practically selective light absorption, only promoting the light scattering effect of dispersed particles in the polymer matrix. Fibres bleached with H_2O_2 produced a selective absorption at a low wavelength, mainly when the SWE extraction was carried out at 170 °C and bleaching was performed with 4% H_2O_2. The PO and 150 fibres provoked similar T_i reductions. In contrast, the 170 fibres produced a more marked reduction of T_i, in line with their lower WI resulting from the greatest formation of brown compounds during the SWE extraction at the highest temperature [7].

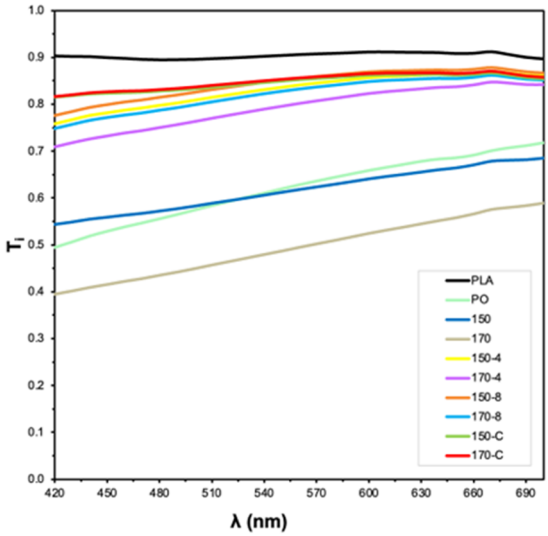

Figure 3. Internal transmittance (T_i) of PLA films with different lignocellulosic fibres.

Therefore, the effect of the lignocellulosic residues on the transparency and colour of the films was affected by the light scattering effect promoted by dispersed particles in the PLA matrix and by the light absorption that occurred in coloured compounds of lignocellulosic particles. Both T_i and L^* increased when fibres were whiter, while the chromatic characteristics (C_{ab}^* and h_{ab}^*) were also affected by the WI of the fibres.

3.2. Barrier Properties of the Films

The water vapour permeability (WVP) and the oxygen permeability (OP) of the different films are shown in Figure 4. The PLA control film exhibited WVP and OP values of 6.34 × 10^{-2} g.mm.kPa^{-1}.h^{-1}.m^{-2} and 1.81 × 1012 cm^3.m^{-1}.s^{-1}.Pa^{-1}, respectively, which are within the range of previously reported values for amorphous PLA films [39–41]. Every lignocellulosic fraction increased the WVP of the PLA films to a different extent, depending on the fibre composition. The samples with the most significant increase were those bleached with 4% H_2O_2 (150-4 and 170-4), whereas the least notable effect occurred in samples containing PO fibres, non-bleached fibres (150 and 170), and chlorite-beached fibres (150-C and 170-C). Therefore, the cellulose content and the presence of other compounds in the fibres affected their influence on the film barrier capacity. Other authors [42,43] also observed an increase in the WVP of PLA films when cellulose fractions were incorporated into the PLA matrix, depending on their ratio. This expected result is due to the hydrophilic nature of the fibres, which contributes negatively to the control of water transfer in the polyester matrix. The fibre particles with a higher affinity for water molecules than the PLA matrix do not introduce an effective tortuosity factor for the transport of water molecules, but enhance their transfer rate in the matrix. The increase in WVP by the fibres will be affected by different factors, such as (1) the cellulose purity and crystallinity degree of the fibres, since mass transport is slower in crystalline phases than in amorphous phases; (2) the ratio of less polar compounds in the fibres, such as lignin, that can decrease their water affinity; (3) the potential diffusion of different low-molecular-weight compounds present in the fibres through the PLA matrix, interacting with the PLA chains and modifying its barrier capacity; and (4) the fibres' morphology (particle size distribution) and surface properties (smoothness and chemical groups at the surface) that would affect their dispersion capacity in the composite matrix and interfacial adhesion. The combination of all these different factors could result in a fibre effect that is difficult to predict on the basis of a single factor, such as the cellulose content.

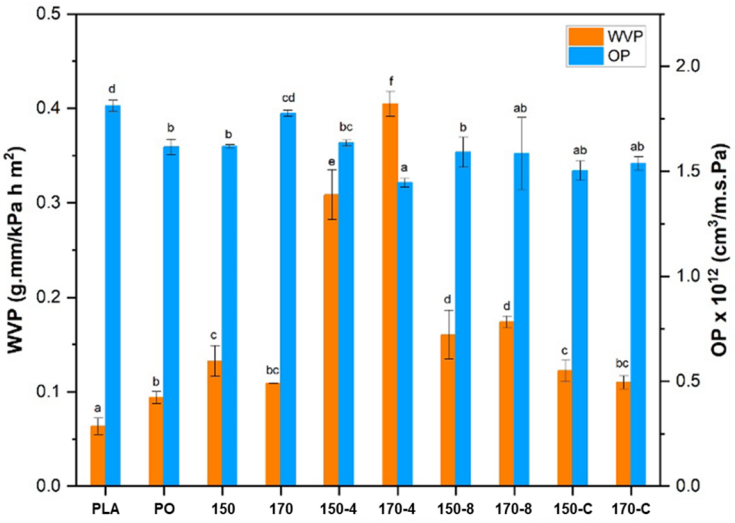

Figure 4. The water vapour permeability (WVP) and oxygen permeability (OP) of the PLA films are affected by lignocellulosic fibre addition. For each barrier property, different letters indicate significant differences among the samples ($p < 0.05$).

As concerns the diffusion of low-molecular-weight compounds from the fibres, phenolic compounds retained in the lignocellulosic matrix or bonded water (values shown in Table 1) could migrate, mainly during the melt-blending process, towards the PLA phase, interacting with the polymer chains and affecting the chain arrangement and subsequent matrix cohesion and physical properties. Specifically, water molecules could provoke the partial hydrolysis of the chains at high temperatures, reducing the cohesion forces of the polymer matrix and their barrier capacity. In this sense, fibres 150-4 and 170-4 provided the films with the greatest WVP and had a relatively high content of bound water in the range of the non-bleached fibres, but these had lower contents of lignin that could mitigate the water transfer through of non-bleached fibres.

As reported in a previous study [7], the morphology of the fibres (particle size distribution and surface properties) were very different, which will greatly influence their dispersion capacity in the polymer matrix and their subsequent effects on the composite's physical properties [44]. Specifically, SWE at 170 °C reduced the particle size of PO particles to a greater extent than SWE at 150 °C, while bleaching with sodium chlorite reduced the particle size more than the treatments with hydrogen peroxide [7]. Likewise, the surface characteristics of the fibres were markedly different depending on the treatment. Fibres obtained at 170 °C and bleached with sodium chlorite (170-C) exhibited the smoothest surface and the highest disaggregation of bundles due to the higher removal of non-cellulosic compounds [7]. Differences in fibre morphology greatly affect the properties of composites [45].

In contrast to the WVP, the presence of lignocellulosic particles provoked a decrease in the OP of PLA films, as also reported by Kumar et al. [43] for PLA films containing cellulosic fillers. The lower oxygen affinity of the hydrophilic fibres increased the tortuous path for the gas molecules to diffuse through the film, acting as a barrier against gas diffusion and reducing oxygen permeability. The lowest reduction occurred in sample 170, and the fibre 170-4 was the one that caused the most significant decrease, whereas the rest of the fibres produced similar reductions. Therefore, the combined effects of the different factors commented on above seem to control the changes in the film barrier properties.

3.3. Mechanical Properties

The film's tensile parameters are shown in Table 3. The elongation at break (EB), tensile strength at break (TS), and elastic modulus (EM) were determined from the stress–strain curves of the tensile test. The incorporation of the fibres provoked changes in the tensile parameters, leading to films that were less extensible and less resistant to break, with

varying values of the elastic modulus (900–3000 MPa). As reported by Mathew et al. [46] for PLA composites with different ratios of microcrystalline cellulose, or Khosravi et al. [33] for PLA composites with different cellulose fractions, the reinforcing effect is mainly reflected in the increase in the EM of PLA films, which was only produced by bleached fibres (mainly for 170-8 and 150-8 samples), except for the fibre 150-4. The 150-4 bleached fibres reduced the EM of the film, which could be attributed not only to the lower cellulose purification efficiency of the applied treatment but also to the larger particle size and aggregated fibre bundles [7], which makes its reinforcing effect less effective. The fibre dimensions, strength, crystallinity, and structure greatly affect the reinforcing action in the composites [45].

Table 3. Elongation at break (EB), tensile strength at break (TS), and elastic modulus (EM) of the different PLA films according to the purification degree of the lignocellulosic residues. Mean values ± standard deviations.

Film	EB (%)	TS (MPa)	EM (MPa)
PLA	5.8 ± 0.9^{f}	43.7 ± 1.2^{e}	1050 ± 80^{b}
PO	4.8 ± 0.4^{e}	37.0 ± 3.0^{d}	930 ± 50^{ab}
150	4.6 ± 0.4^{de}	36.0 ± 5.0^{cd}	930 ± 40^{ab}
170	4.2 ± 0.5^{cd}	32.0 ± 5.0^{b}	950 ± 50^{ab}
150-4	4.0 ± 0.6^{c}	38.0 ± 2.0^{d}	900 ± 60^{a}
170-4	0.7 ± 0.3^{a}	8.0 ± 3.0^{a}	1390 ± 140^{c}
150-8	3.1 ± 0.4^{b}	38.0 ± 5.0^{d}	1530 ± 130^{d}
170-8	1.2 ± 0.1^{a}	33.0 ± 4.0^{bc}	3300 ± 200^{e}
150-C	3.1 ± 0.3^{b}	38.0 ± 2.0^{d}	1300 ± 120^{c}
170-C	3.4 ± 0.2^{b}	43.0 ± 3.0^{e}	1300 ± 130^{c}

Different letters in the same column indicate significant differences among the samples ($p < 0.05$).

The non-bleached fractions (PO, 150, and 170) did not produce a significant reinforcing effect, probably due to their lower richness in cellulose (Table 1). These non-bleached fibres reduced the EM and TS without remarkable changes in the film stretchability. The lower strength of non-bleached fibres due to the high content of amorphous components, such as hemicellulose and lignin, and their bigger size can contribute to their lack of capacity to transfer force in the composites. The reinforcing effect is related to the mechanical stiffness and crystallinity of the filler, the interfacial adhesion of the fibre and polymer, and the involved force transmission mechanisms within the composite, depending on the structural arrangement [47]. Nevertheless, for fillers with a complex composition, other factors previously commented must be considered, such as the potential changes in the polymer chains promoted by the incorporation of hygroscopic particles and the specific interactions of the polymer with potential compounds that diffused from the fibres. Hydrophilic materials usually contain bonded water that can be released during melt blending with the polymer. At high temperatures, the release of water molecules can induce the partial hydrolysis of the polyester molecules, thus reducing the cohesive forces in the polymer matrix and affecting the tensile behaviour. In this sense, bleached fibres, with a lower ratio of amorphous fraction, have a lower water binding capacity (as shown in Table 1) and fewer possibilities to promote the hydrolysis of PLA chains. Likewise, low-molecular-weight compounds, such as phenolic acids, present in the lignocellulosic fractions can interact with the PLA chains, modifying the tensile behaviour of the matrix. In this sense, different studies have reported a cross-linking effect of some phenolic hydroxyls and polyester carbonyl [40,48].

3.4. Thermal Behaviour

The changes induced by the lignocellulosic fibres in the thermal stability and the glass transition of the amorphous PLA were evaluated by TGA and DSC. Figure 5 shows the TGA and the DTGA curves obtained for the different PLA composite films. The TGA curves of the films show the typical single degradation step described for PLA, with no

significant effect of the fibres on the curve pattern due to their relatively low mass ratio in the films. The temperature of the maximum degradation rate (T_{peak} in DTGA curves) of amorphous PLA was 362 °C, which is within the previously reported range [39,40]. However, a decrease in this T_{peak} was observed for films containing fibres, depending on their composition. The maximum decrease was observed for the 170-4 sample (ΔT = 55 °C), whereas sample 170-C showed the lowest shift (ΔT = 8 °C), and a nearly 30 °C decrease was observed for films with non-bleached fibres (150 and 170) and 150-4 fibres. Nguyen et al. [49] also found this decrease in cellulose-PLA composites, which was attributed to the water-binding capacity of the cellulose fibres that can accelerate the biocomposites' water absorption, leading to a decrease in thermal stability. However, no significant correlation between the T_{peak} decrease and the content of bonded water of the fibres was observed, suggesting that other polymer interactions with different compounds that migrated from the fibres could play an essential role in the loss of the thermal stability of the material. In fact, the strong effect of fibres in the 170-4 film is remarkable despite the high purity of cellulose (80%) and the relatively low content of bonded water.

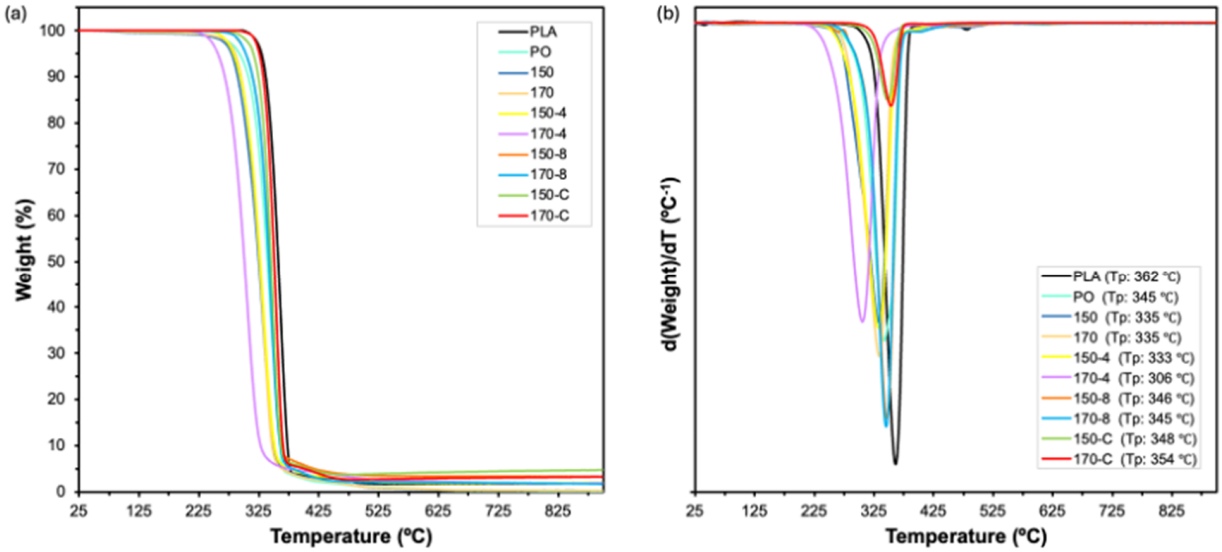

Figure 5. (**a**) Thermogravimetric analysis (TGA) curves and (**b**) first derivative (DTGA) curves of the PLA films with the different lignocellulosic residues.

Figure 6 shows the first and second heating scans of the different PLA films, indicating the T_g values (mid-point) obtained in each case. For a determined sample, even for net PLA, slight differences in the T_g values were observed in the first and second scans, where the values of the former were always slightly greater, which can be attributable to the thermal history and aging of the material. Considering the T_g values of the second scan when the thermal history was erased, a significant decrease (ΔT_g: 3–4 °C) in the T_g values of composites relative to the net PLA was only observed in samples containing PO or 170 fibres. The latter suggests that some compounds of these non-purified fibres could migrate into the polymer matrix, provoking a certain plasticising effect. Frone et al. [50] reported that the T_g measured by DSC is not sensitive enough to detect modifications in the restriction of PLA mobility provoked by nanofillers since the low content of nanofillers only involves a small fraction of the PLA chains. Similar effects can be expected for microfillers, such as the cellulosic fractions in the present study.

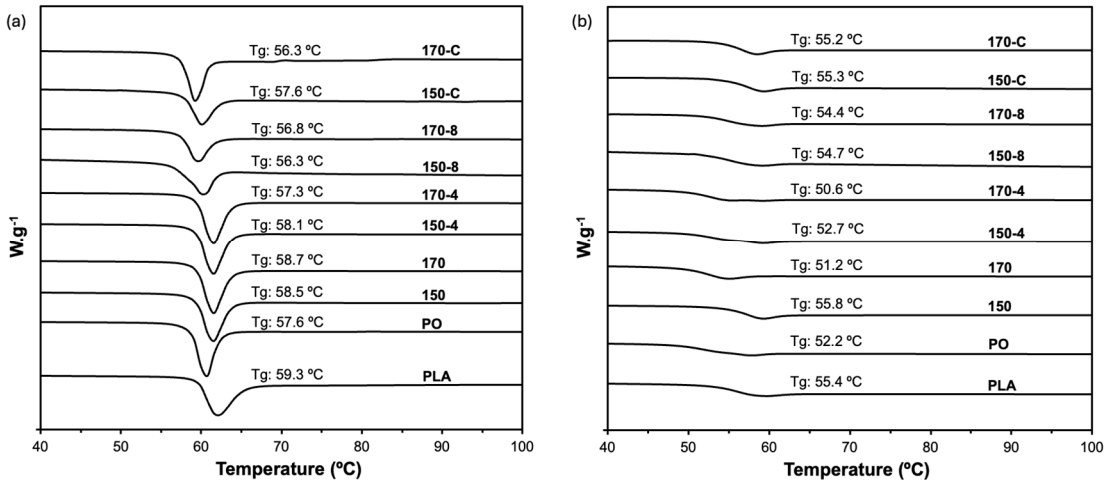

Figure 6. First (**a**) and second (**b**) heating DSC thermograms of PLA films with the different lignocellulosic fractions.

3.5. Microstructural Properties of the Films

The arrangement of the fibres in the PLA matrix was observed through the HRFESEM images of the cross-sections of the PLA composites (Figure 7). The PLA control film exhibited a typical homogeneous surface, with brittle and rubbery fracture, as previously observed by other authors [39,51]. In the composites, the fibres were well dispersed in the polymer matrix and exhibited good interfacial adhesion, as deduced from the absence of fibre separation from the matrix during the film cryofracture. Likewise, no qualitative differences regarding the degree of integration in the matrix could be detected for the fibres with different compositions. Nevertheless, the above-commented differences in the particle size distribution reported for these fibres [7] are reflected in the micrographs of the different composites. Likewise, the different tendencies to aggregate the fibres could lead to different dispersion degrees of the fibres in the composites. Fibres bleached with hydrogen peroxide and sodium chlorite exhibited different surface morphologies that were attributed to the different oxidative mechanisms of the bleaching agent, which alter the cellulosic fibres to different extents [7]. Bleaching agents act by oxidizing and degrading lignin, effectively removing it from the fibre structure and exposing more of the cellulose within the fibre while the fibre surface becomes smoother and cleaner, enhancing its potential to interact with polymer matrices. Sari et al. [44] reported that fibre surface treated with $NaClO_2$ had improved adhesion to the polymer matrix. In contrast, bleaching with hydrogen peroxide may provoke an alteration of cellulose through oxidative mechanisms based on the generation of alpha hydroxyalkyl radicals, as described by Vismara et al. [52], which may modify the surface energy of the fibres. Therefore, the different treatments applied to the fibres implied the modification of their overall composition, size, and shape, and surface properties due to the different degrees of elimination of non-cellulosic compounds from the fibres' performance [45]. It is expected that reducing the hemicellulose and lignin concentrations through the actions of the different treatments enhance the fibres' performance.

The particle size and the bounding forces at the fibre–polymer interface greatly affect the mechanical performance of the composites [53]. Therefore, the differences in the particle size and adhesion forces could contribute to explaining their different effects on the composite tensile behaviour. Better dispersion of bleached fibres and interfacial adhesion forces could be expected due to the greater cellulose purity. Nevertheless, the presence of more hydrophobic compounds on the fibre surface could contribute to the good integration of non-bleached materials in the hydrophobic PLA. In fact, composites of bleached fibres exhibited greater elastic modulus values than net PLA but also had lower extensibility and resistance to fracture, mainly the 170-4 and 170-8 films, which were very brittle. In contrast,

non-bleached fibres reduced the elastic modulus of PLA but did not exhibit such notable losses in the films' stretchability and resistance to break.

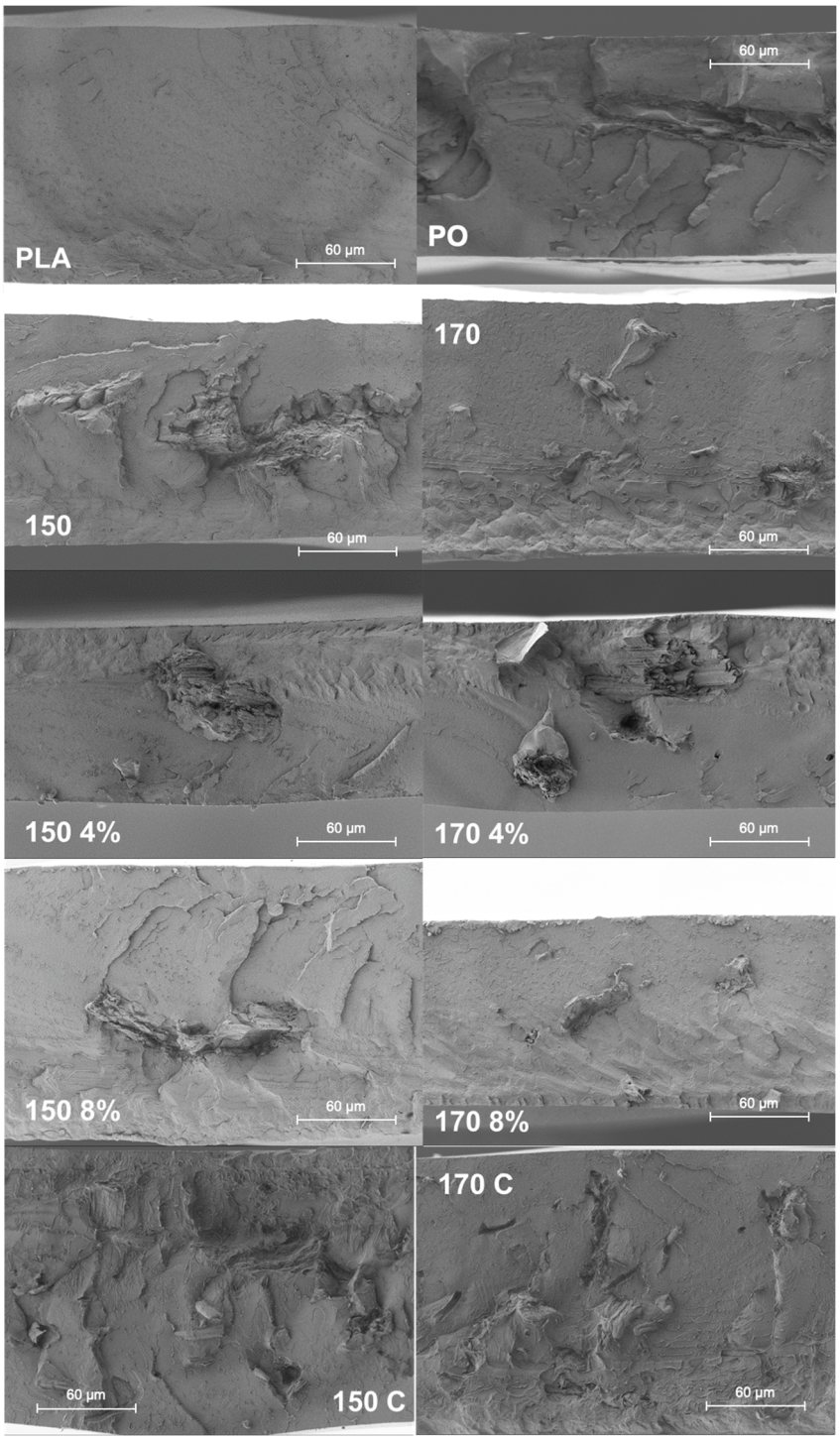

Figure 7. HRFESEM images (×450) of the cross-sections of PLA films with the different incorporated lignocellulosic residues.

4. Conclusions

PLA composite films with lignocellulosic fibres from *Posidonia oceanica* waste were successfully obtained from melt blending and compression moulding. The properties of composites were highly affected by the fibre treatment (SWE temperature and kind or concentration of bleaching agent). The non-bleached fibres greatly reduced the film's

lightness and transparency, affecting the chromatic appearance as a function of their brown colour. Bleached fibres gave rise to lighter and more transparent films, depending on their final whiteness. Thus, the chlorite-bleached fibres had the lowest optical impact on the PLA films. All fibres reduced the water barrier capacity of PLA films while enhancing the oxygen barrier, depending on the applied treatment and its effect on the fibre composition and morphology. Only bleached fibres had a reinforcing effect on composites, promoting their stiffness and reducing their extensibility and resistance to break, with 170-C fibres being those that reduced the film ductility the least. The non-bleached fibres decreased the elastic modulus (10%), extensibility (17%), and tensile at break (20%) to a similar extent. Therefore, for food packaging uses, the 170-C fibres would be recommended to obtain colourless and transparent PLA films with the best mechanical and barrier performance. In contrast, if transparency and colour are not limiting for food uses, the incorporation of untreated PO fibres allowed for good preservation of the PLA water vapour barrier capacity, enhanced the oxygen barrier, and provided the films with a similar tensile behaviour to the other non-bleached fractions. This approach, without any treatment to purify the cellulose, would be the most suitable and cheapest approach to obtain coloured composites films. Further studies are needed to optimise the fibre ratio while minimising the material cost, considering the direct use of untreated PO fibres to obtain coloured films or 170-C fibres to obtain colourless and more transparent films.

Author Contributions: Conceptualization, P.A.V.F., C.G.-M., A.C. and M.V.; methodology, P.C.-B., P.A.V.F., C.G.-M., A.C. and M.V.; formal analysis, P.C.-B., P.A.V.F., C.G.-M., A.C. and M.V.; investigation, P.C.-B. and P.A.V.F.; resources, C.G.-M., A.C. and M.V.; data curation, P.C.-B., P.A.V.F. and C.G.-M.; writing—original draft preparation, C.G.-M., P.C.-B., P.A.V.F., A.C. and M.V.; writing—review and editing, P.C.-B., P.A.V.F., C.G.-M., A.C. and M.V.; supervision, C.G.-M., M.V. and A.C.; project administration, C.G.-M. and A.C.; funding acquisition, C.G.-M., A.C. and M.V. All authors have read and agreed to the published version of the manuscript.

Funding: This research was funded by Agencia Estatal de Investigación of Spain through the Project TED2021-132295B-I00 and by Generalitat Valenciana (Project CIPROM/2021/071).

Institutional Review Board Statement: Not applicable.

Data Availability Statement: The raw data supporting the conclusions of this article will be made available by the authors upon request.

Conflicts of Interest: The authors declare no conflicts of interest.

References

1. Pergent, G.; Rico-Raimondino, V.; Pergent-Martini, C. Fate of Primary Production in *Posidonia Oceanica* Meadows of the Mediterranean. *Aquat. Bot.* **1997**, *59*, 307–321. [CrossRef]
2. Tranchina, L.; Miccichè, S.; Bartolotta, A.; Brai, M.; Mantegna, R.N. *Posidonia Oceanica* as a Historical Monitor Device of Lead Concentration in Marine Environment. *Environ. Sci. Technol.* **2005**, *39*, 3006–3012. [CrossRef] [PubMed]
3. Pergent-Martini, C.; Pergent, G.; Monnier, B.; Boudouresque, C.-F.; Mori, C.; Valette-Sansevin, A. Contribution of *Posidonia Oceanica* Meadows in the Context of Climate Change Mitigation in the Mediterranean Sea. *Mar. Environ. Res.* **2021**, *165*, 105236. [CrossRef] [PubMed]
4. Litsi-Mizan, V.; Efthymiadis, P.T.; Gerakaris, V.; Serrano, O.; Tsapakis, M.; Apostolaki, E.T. Decline of Seagrass (*Posidonia oceanica*) Production over Two Decades in the Face of Warming of the Eastern Mediterranean Sea. *New Phytol.* **2023**, *239*, 2126–2137. [CrossRef] [PubMed]
5. Cocozza, C.; Parente, A.; Zaccone, C.; Mininni, C.; Santamaria, P.; Miano, T. Chemical, Physical and Spectroscopic Characterization of *Posidonia oceanica* (L.) Del. Residues and Their Possible Recycle. *Biomass Bioenergy* **2011**, *35*, 799–807. [CrossRef]
6. *European Seagrasses: An Introduction to Monitoring and Management*; Borum, J., Duarte, C.M., Krause-Jensen, D., Greve, T.M., Eds.; The M&MS Project S. L.: Hillerød, Denmark, 2004; ISBN 978-87-89143-21-7.
7. Camarena-Bononad, P.; Freitas, P.A.V.; Chiralt, A.; Vargas, M. Subcritical Water Extraction for Recovering Cellulose Fibres from *Posidonia oceanica* Waste. *Carbohydr. Polym. Technol. Appl.* **2024**, *8*, 100550. [CrossRef]
8. Bettaieb, F.; Khiari, R.; Hassan, M.L.; Belgacem, M.N.; Bras, J.; Dufresne, A.; Mhenni, M.F. Preparation and Characterization of New Cellulose Nanocrystals from Marine Biomass *Posidonia Oceanica*. *Ind. Crops Prod.* **2015**, *72*, 175–182. [CrossRef]

9. Khiari, R.; Mhenni, M.F.; Belgacem, M.N.; Mauret, E. Chemical Composition and Pulping of Date Palm Rachis and *Posidonia Oceanica*—A Comparison with Other Wood and Non-Wood Fibre Sources. *Bioresour. Technol.* **2010**, *101*, 775–780. [CrossRef] [PubMed]
10. Ncibi, M.C.; Jeanne-Rose, V.; Mahjoub, B.; Jean-Marius, C.; Lambert, J.; Ehrhardt, J.J.; Bercion, Y.; Seffen, M.; Gaspard, S. Preparation and Characterisation of Raw Chars and Physically Activated Carbons Derived from Marine *Posidonia oceanica* (L.) Fibres. *J. Hazard. Mater.* **2009**, *165*, 240–249. [CrossRef]
11. Czaja, W.K.; Young, D.J.; Kawecki, M.; Brown, R.M. The Future Prospects of Microbial Cellulose in Biomedical Applications. *Biomacromolecules* **2007**, *8*, 1–12. [CrossRef]
12. Verdini, F.; Calcio Gaudino, E.; Grillo, G.; Tabasso, S.; Cravotto, G. Cellulose Recovery from Agri-Food Residues by Effective Cavitational Treatments. *Appl. Sci.* **2021**, *11*, 4693. [CrossRef]
13. Ruthes, A.C.; Martínez-Abad, A.; Tan, H.-T.; Bulone, V.; Vilaplana, F. Sequential Fractionation of Feruloylated Hemicelluloses and Oligosaccharides from Wheat Bran Using Subcritical Water and Xylanolytic Enzymes. *Green Chem.* **2017**, *19*, 1919–1931. [CrossRef]
14. Cheng, Y.; Xue, F.; Yu, S.; Du, S.; Yang, Y. Subcritical Water Extraction of Natural Products. *Molecules* **2021**, *26*, 4004. [CrossRef] [PubMed]
15. Zhang, J.; Wen, C.; Zhang, H.; Duan, Y.; Ma, H. Recent Advances in the Extraction of Bioactive Compounds with Subcritical Water: A Review. *Trends Food Sci. Technol.* **2020**, *95*, 183–195. [CrossRef]
16. Farhat, W.; Venditti, R.; Quick, A.; Taha, M.; Mignard, N.; Becquart, F.; Ayoub, A. Hemicellulose Extraction and Characterization for Applications in Paper Coatings and Adhesives. *Ind. Crops Prod.* **2017**, *107*, 370–377. [CrossRef]
17. Ng, H.-M.; Sin, L.T.; Tee, T.-T.; Bee, S.-T.; Hui, D.; Low, C.-Y.; Rahmat, A.R. Extraction of Cellulose Nanocrystals from Plant Sources for Application as Reinforcing Agent in Polymers. *Compos. Part B Eng.* **2015**, *75*, 176–200. [CrossRef]
18. Freitas, P.A.V.; Santana, L.; González-Martínez, C.; Chiralt, A. Combining Subcritical Water Extraction and Bleaching with Hydrogen Peroxide to Obtain Cellulose Fibres from Rice Straw. *Carbohydr. Polym. Technol. Appl.* **2024**, *7*, 100491. [CrossRef]
19. Li, L.; Lee, S.; Lee, H.L.; Youn, H.J. Hydrogen Peroxide Bleaching of Hardwood Kraft Pulp with Adsorbed Birch Xylan and Its Effect on Paper Properties. *BioRes* **2011**, *6*, 721–736. [CrossRef]
20. Hong, L.G.; Yuhana, N.Y.; Zawawi, E.Z.E. Review of Bioplastics as Food Packaging Materials. *AIMS Mater. Sci.* **2021**, *8*, 166–184. [CrossRef]
21. Naser, A.Z.; Deiab, I.; Darras, B.M. Poly(Lactic Acid) (PLA) and Polyhydroxyalkanoates (PHAs), Green Alternatives to Petroleum-Based Plastics: A Review. *RSC Adv.* **2021**, *11*, 17151–17196. [CrossRef]
22. Siakeng, R.; Jawaid, M.; Ariffin, H.; Sapuan, S.M.; Asim, M.; Saba, N. Natural Fiber Reinforced Polylactic Acid Composites: A Review. *Polym. Compos.* **2019**, *40*, 446–463. [CrossRef]
23. Sudamrao Getme, A.; Patel, B. A Review: Bio-Fiber's as Reinforcement in Composites of Polylactic Acid (PLA). *Mater. Today: Proc.* **2020**, *26*, 2116–2122. [CrossRef]
24. Li, X.; Lin, Y.; Liu, M.; Meng, L.; Li, C. A Review of Research and Application of Polylactic Acid Composites. *J. Appl. Polym. Sci.* **2023**, *140*, e53477. [CrossRef]
25. Elsawy, M.A.; Kim, K.-H.; Park, J.-W.; Deep, A. Hydrolytic Degradation of Polylactic Acid (PLA) and Its Composites. *Renew. Sustain. Energy Rev.* **2017**, *79*, 1346–1352. [CrossRef]
26. Scaffaro, R.; Maio, A.; Lopresti, F. Physical Properties of Green Composites Based on Poly-Lactic Acid or Mater-Bi® Filled with *Posidonia Oceanica* Leaves. *Compos. Part A Appl. Sci. Manuf.* **2018**, *112*, 315–327. [CrossRef]
27. Scaffaro, R.; Lopresti, F.; Botta, L. PLA Based Biocomposites Reinforced with *Posidonia Oceanica* Leaves. *Compos. Part B Eng.* **2018**, *139*, 1–11. [CrossRef]
28. Scaffaro, R.; Maio, A.; Gammino, M. Hybrid Biocomposites Based on Polylactic Acid and Natural Fillers from Chamaerops Humilis Dwarf Palm and *Posidonia Oceanica* Leaves. *Adv. Compos. Hybrid. Mater.* **2022**, *5*, 1988–2001. [CrossRef]
29. Barandiaran, A.; Lascano, D.; Montanes, N.; Balart, R.; Selles, M.A.; Moreno, V. Improvement of the Ductility of Environmentally Friendly Poly(Lactide) Composites with *Posidonia Oceanica* Wastes Plasticized with an Ester of Cinnamic Acid. *Polymers* **2023**, *15*, 4534. [CrossRef]
30. Slimani, F.; Ghanmi, I.; Ghanmi, S.; Guedri, M. Production of Thermoplastic Composites Reinforced with *Posidonia Oceanica* Fibers. *Eng. Technol. Appl. Sci. Res.* **2024**, *14*, 13243–13247. [CrossRef]
31. Sathish, S.; Aravindh, M.; Gokulkumar, S.; Dharani Kumar, S.; Prabhu, L.; Raj, R.R. Interface Engineering-Matrix Modification in Cellulose Fiber Composites. In *Cellulose Fibre Reinforced Composites*; Elsevier: Amsterdam, The Netherlands, 2023; pp. 95–114. ISBN 978-0-323-90125-3.
32. Sluiter, A. *Determination of Structural Carbohydrates and Lignin in Biomass: Laboratory Analytical Procedure (LAP)*; Issue Date: 7/17/2005. Technical Report; NREL: Wahington, DC, USA, 2008.
33. Khosravi, A.; Fereidoon, A.; Khorasani, M.M.; Naderi, G.; Ganjali, M.R.; Zarrintaj, P.; Saeb, M.R.; Gutiérrez, T.J. Soft and Hard Sections from Cellulose-Reinforced Poly(Lactic Acid)-Based Food Packaging Films: A Critical Review. *Food Packag. Shelf Life* **2020**, *23*, 100429. [CrossRef]
34. Freitas, P.A.V.; Arias, C.I.L.F.; Torres-Giner, S.; González-Martínez, C.; Chiralt, A. Valorization of Rice Straw into Cellulose Microfibers for the Reinforcement of Thermoplastic Corn Starch Films. *Applied Sciences* **2021**, *11*, 8433. [CrossRef]

35. *ASTM E96/E96M-05*; Standard Test Methods for Water Vapor Transmission of Materials. American Society for Testing and Materials: West Conshohocken, PA, USA, 2005; pp. 1–11.
36. *ASTM D3985-05*; Oxygen Gas Transmission Rate Through Plastic Film and Sheeting Using a Coulometric Sensor. Annual Book of ASTM Standards, C. American Society for Testing and Materials: West Conshohocken, PA, USA, 2010; pp. 1–7.
37. *ASTM D882-12*; Standard Test Method for Tensile Properties of thin Plastic Sheeting. American Society for Testing and Materials: West Conshohocken, PA, USA, 2012; p. 12.
38. Fortunati, E.; Luzi, F.; Puglia, D.; Petrucci, R.; Kenny, J.M.; Torre, L. Processing of PLA Nanocomposites with Cellulose Nanocrystals Extracted from *Posidonia oceanica* Waste: Innovative Reuse of Coastal Plant. *Ind. Crops Prod.* **2015**, *67*, 439–447. [CrossRef]
39. Freitas, P.A.V.; Bas Gil, N.J.; González-Martínez, C.; Chiralt, A. Antioxidant Poly (Lactic Acid) Films with Rice Straw Extract for Food Packaging Applications. *Food Packag. Shelf Life* **2022**, *34*, 101003. [CrossRef]
40. Ordoñez, R.; Atarés, L.; Chiralt, A. Effect of Ferulic and Cinnamic Acids on the Functional and Antimicrobial Properties in Thermo-Processed PLA Films. *Food Packag. Shelf Life* **2022**, *33*, 100882. [CrossRef]
41. Drieskens, M.; Peeters, R.; Mullens, J.; Franco, D.; Lemstra, P.J.; Hristova-Bogaerds, D.G. Structure versus Properties Relationship of Poly(Lactic Acid). I. Effect of Crystallinity on Barrier Properties. *J. Polym. Sci. B Polym. Phys.* **2009**, *47*, 2247–2258. [CrossRef]
42. Abdulkhani, A.; Hosseinzadeh, J.; Dadashi, S.; Mousavi, M. A study of morphological, thermal, mechanical and barrier properties of pla based biocomposites prepared with micro and nano sized cellulosic fibers. *Cellul. Chem. Technol.* **2015**, *49*, 597–605.
43. Kumar, R.; Kumari, S.; Rai, B.; Das, R.; Kumar, G. Effect of Nano-Cellulosic Fiber on Mechanical and Barrier Properties of Polylactic Acid (PLA) Green Nanocomposite Film. *Mater. Res. Express* **2019**, *6*, 125108. [CrossRef]
44. Sari, N.H.; Sari, S.; Sutaryono, Y.A.; Khan, M.A. A Review: Fracture Structure of Natural Fiber Surface after Treatment with Various Alkali Chemicals. *J. Fibers Polym. Compos.* **2024**, *3*, 158–180.
45. Pereira, P.H.F.; Rosa, M.D.F.; Cioffi, M.O.H.; Benini, K.C.C.D.C.; Milanese, A.C.; Voorwald, H.J.C.; Mulinari, D.R. Vegetal Fibers in Polymeric Composites: A Review. *Polímeros* **2015**, *25*, 9–22. [CrossRef]
46. Mathew, A.P.; Oksman, K.; Sain, M. Mechanical Properties of Biodegradable Composites from Poly Lactic Acid (PLA) and Microcrystalline Cellulose (MCC). *J. Appl. Polym. Sci.* **2005**, *97*, 2014–2025. [CrossRef]
47. Graupner, N.; Herrmann, A.S.; Müssig, J. Natural and Man-Made Cellulose Fibre-Reinforced Poly(Lactic Acid) (PLA) Composites: An Overview about Mechanical Characteristics and Application Areas. *Compos. Part A Appl. Sci. Manuf.* **2009**, *40*, 810–821. [CrossRef]
48. Hernández-García, E.; Vargas, M.; Chiralt, A. Effect of Active Phenolic Acids on Properties of PLA-PHBV Blend Films. *Food Packag. Shelf Life* **2022**, *33*, 100894. [CrossRef]
49. Nguyen, T.C.; Ruksakulpiwat, C.; Ruksakulpiwat, Y. Effect of Cellulose Nanofibers from Cassava Pulp on Physical Properties of Poly(Lactic Acid) Biocomposites. *J. Thermoplast. Compos. Mater.* **2020**, *33*, 1094–1108. [CrossRef]
50. Frone, A.N.; Berlioz, S.; Chailan, J.-F.; Panaitescu, D.M. Morphology and Thermal Properties of PLA–Cellulose Nanofibers Composites. *Carbohydr. Polym.* **2013**, *91*, 377–384. [CrossRef] [PubMed]
51. Muller, J.; González-Martínez, C.; Chiralt, A. Poly(Lactic) Acid (PLA) and Starch Bilayer Films, Containing Cinnamaldehyde, Obtained by Compression Moulding. *Eur. Polym. J.* **2017**, *95*, 56–70. [CrossRef]
52. Vismara, E.; Gastaldi, G.; Valerio, A.; Bertini, S.; Cosentino, C.; Eisle, G. Alpha Cellulose from Industrial and Agricultural Renewable Sources like Short Flax Fibres, Ears of Corn and Wheat-Straw and Its Transformation into Cellulose Acetates. *J. Mater. Chem.* **2009**, *19*, 8678. [CrossRef]
53. Rasheed, M.; Jawaid, M.; Parveez, B. Preparation, Characterization and Properties of Biodegradable Composites from Bamboo Fibers—Mechanical and Morphological Study. *J. Polym. Environ.* **2021**, *29*, 4120–4126. [CrossRef]